Single-cell behavior

Quantitative Biology

From Molecular to Cellular Systems

Part III: Quantitative Methods

Chapter 8: Single-cell behavior

Philippe Cluzel

Center for Systems Biology, Department of Molecular and Cellular Biology, and School of Engineering and Applied Sciences, Harvard University; Northwest Labs Building, 52 Oxford St Cambridge, MA 02138

Introduction

Studying random fluctuations to characterize the properties of dynamical systems has been a classic approach of condensed matter physics and has more recently been extended to economics and biology. Historically, this field of research was prompted by the observation of what is known today as Brownian motion. In 1827, botanist Robert Brown used an optical microscope to observe that when pollen from *Clarckia pulchella* was suspended in water, individual grains within the pollen displayed jittery movements (1). He further demonstrated that the observed random motion was not due to the presence of 'living' animalcules within the pollen, because the motion was also observed in microscopic examinations of fossilized wood and dust (1). Since this early observation of Brownian motion, there has been a steady stream of studies on this subject, but the first key conceptual advancement came from Albert Einstein in a 1905 paper (2) that predicted that the mean square displacement of a Brownian particle was proportional to the time of observation. Einstein assumed that the motion of a Brownian particle is governed by the temperature of the fluid, which produces a random force and the friction of the fluid on the particle. These assumptions yield the classic formula of diffusion that gives the mean square distance covered by a Brownian particle during a given time interval as $\left\langle \delta x^2 \right\rangle_N = D\tau$, where D is the diffusion constant that depends on the temperature and the friction of the fluid. This formula emphasizes that some relevant information about the stochastic variable $\delta x(t)$ defined with $x(t) = \left\langle x \right\rangle_{Time} + \delta x(t)$ is obtained by characterizing its second moment (i.e. variance).

Here we bring Brownian motion back to biology. Most of the themes discussed in this chapter illustrate how the concept of the Brownian particle and the measure of its associated mean square displacement can be used directly to extract intracellular biochemical parameters from individual

living cells. The literature on this subject is vast, and I purposely selected only few examples for the sake of simplicity and cohesiveness, focusing exclusively on bacteria. The intent of this chapter is not to present an exhaustive review of the subject, but rather to discuss several methods that may be useful for characterizing the behavior of individual cells.

First, we will describe the principles and latest developments of fluorescence correlation spectroscopy (FCS). This technique is based on monitoring the fluctuations of the fluorescence signal associated with dyes that diffuse in and out a small volume of detection (3-5). We will discuss the specific application developed to measure coding and non-coding RNAs in individual living bacteria (6-7).

Second, we will introduce the well-known stochastic Langevin equation that describes the motion of a Brownian particle in the limit of low Reynolds number. We will discuss how the same phenomenological stochastic equation has been successfully used to model and characterize cell-to-cell variability in the expression of a single gene in bacteria (8). Thus far, most of the studies have focused on the static distribution of the cell-to-cell variability within an isogenic population (8-9). However, we will extend the discussion to the dynamic aspect of variability and we will desrcibe how the analysis of temporal fluctuations of cellular behavior can be used to determine intracellular biochemical parameters (10). Finally, the Langevin equation makes predictions about the linear response of dynamical systems to a small external perturbation. While this phenomenological equation has been used to describe physical systems at thermodynamic equilibrium, we will show that this framework can also be extended to living cells. This extension is possible when the system exhibits a well-defined steady-state and has Markovian dynamics (11). Under Markovian dynamics, the system has a short memory and can relax to a well-defined steady-state. However, this framework is particularly relevant to study

energy consuming mechanisms that are present in the living cells (12). In this chapter, we will discuss the usefulness of this approach to characterize the existence of a fundamental interdependence between spontaneous fluctuations in living cells and their response to a small external stimulus. For non-equilibrium systems, such as living cells, this relationship between fluctuation and response has been recently formalized in a fluctuation-response theorem by (11).

While this theorem predicts the existence of a coupling between fluctuation and response, it does not reveal how this coupling varies as a function of the system parameters, such as gene expression or reaction rates. Therefore, it would be interesting to discuss under what circumstances biological systems would exhibit similar coupling. This approach predicts constraints between variability and response to environmental changes in specific classes of biological systems. We illustrate the usefulness of this theorem using chemotaxis in E. coli as experimental system. We will re-interpret the fluctuation-response theorem and the Langevin equation to highlight the existence of this fundamental relationship between behavioral variability and the response to a small chemotactic stimulus in single bacteria. Subsequently, we will report the design principle in chemotaxis shared by other biological systems, which determines the coupling between response and fluctuations.

1 Fluorescence Correlation Spectroscopy (FCS)

In characterizing the diffusion of fluorescent molecules in solution, Magde, Elson, and Webb, pioneered and developed a new quantitative technique for biology called FCS (3-5). The principle of this technique consists of measuring the fluorescence signal emitted from molecules diffusing freely in and out of a confocal volume of detection. The fluorescence intensity

fluctuates because individual molecules are entering and leaving the volume of detection defined by a diffraction limited laser spot. A normalized autocorrelation function is used to analyze the fluctuations δn of emitted photons (i.e. fluorescence intensity),

$$G(t) = \frac{\langle \delta n(t') \delta n(t'+t) \rangle}{\langle n \rangle^2} \qquad [1]$$

The function G(t) depends on the shape of the illumination profile that is generally Gaussian. In this section, we will focus only on 2-D diffusion. (For a detailed review of the mathematical derivations of the function G(t) see Krichevsky and Bonnet (13).) While 2-D diffusion involves fewer parameters and can be a good approximation for 3-D diffusion, it is also well-suited to examine the diffusion of fluorescent markers in rod-like bacterial cells, such as *E. coli*. If we neglect the diffusion of molecules along the z-axis, G(t) can be simplified to:

$$G(t) = \frac{1}{N}\left(\frac{1}{\left(1 + t/\xi_{free}\right)}\right) \qquad [2]$$

where N is the number of fluorescent particles per detection volume and ξ_{free} is the typical diffusion time of these particles through the detection volume. Fitting the experimental autocorrelation function with G(t) yields the number of molecules present on average in the volume of detection and the diffusion coefficient of the molecules, which depends on their size and the viscosity of their environment.

The power of this approach lies in the fact that the measurements are self-calibrated because they characterize the fluctuations of fluorescence relative to the mean fluorescence signal. Thus, the result does not depend on the intensity of the excitation light. Of course, there are several important limitations to this approach. First, fluctuations in the emitted fluorescence signal must

be large enough relative to the mean. This condition restricts the technique to low concentration of fluorescent markers. For example, the definition of the autocorrelation function becomes poor when there are more than 1000 molecules per effective volume of detection of ~0.1fl. Second, the technique is sensitive to bleaching, which introduces correlations in the fluctuations of intensity and introduces artifacts in the measurements. Third, if molecules are localized and cannot diffuse freely, then FCS does not work. Despite these limitations, FCS has proven to be a powerful tool in single-cell measurements (14-16).

1.1 Measuring intracellular protein diffusion in single bacteria

While FCS was initially developed to measure small traces of dyes in solution (4), it has more recently been applied to living single cells (17). This technique became less invasive with the use of genetically encoded fluorescent proteins (6-7). Using FCS, one of the first examples of the direct quantification of protein concentration within single living cells revealed that the bacterial motor in *E. coli* exhibits an extremely steep input-output sigmoid relationship with a Hill coefficient of about 10 (16). This result is specific to the single-cell approach because when the same bacterial motor was characterized at the population level, it had an input-output relationship that was much smoother with a Hill coefficient of ~ 3 (18-20). To understand this discrepancy, it is important to note that that there exists a strict relationship between the motor behavior and the concentration of a specific signaling protein that controls the motor behavior. When standard ensemble techniques are used to evaluate protein concentration, such as immunoblotting, they ignore the inherent cell-to-cell variability. As a result, ensemble average effectively smoothed out the typical motor characteristics, leading to lower values of the Hill coefficient.

1.2 Measuring intracellular diffusion of RNA in single bacteria

In addition to measuring protein concentration, FCS has been extended to quantify coding and non-coding RNA in single cells (6-7). To label RNA, it is common to use the MS2 labeling system originally developed for yeast by Bertrand and colleagues (21) and subsequently adapted to *E. coli* (22). This system employs two gene constructs encoded on plasmids: a fusion of the RNA-binding MS2 coat protein and GFP (MS2-GFP) and a 23-nucleotide *ms2* RNA binding site (*ms2*-binding site) located downstream of a gene on an RNA transcript. MS2-GFP can either diffuse freely through the cell or bind to the *ms2*-binding sites on the transcript. There are two ms2-binding sites and each site binds an MS2-GFP homodimer. To monitor temporal variations in RNA concentration in real-time, it is essential to account for the slow maturation time of GFP and thus to pre-express MS2-GFP. Free MS2-GFP fusion proteins diffuse through the detection volume (diffraction limited laser spot) with a typical time of ~ 1 ms. The sensitivity of detection of non-coding RNA is increased by fusing a ribosomal binding site to the tandem of *ms2*-binding sites, which produces an RNA/MS2-GFP/ribosome complex that diffuses with a typical diffusion time of ~ 30 ms, 30-fold slower than free MS2-GFP in the cytoplasm. These measurements have high temporal resolution, requiring only a 2-second acquisition time to obtain a reliable autocorrelation function.

To determine the concentration of bound GFP molecules and, therefore, the concentration of the RNA transcripts labeled with MS2 coat proteins, the original autocorrelation function (Equation [2]) is extended to Formula [3a] (13). This new formula takes into account the fact that there is a mixture of bound and free molecules in the detection volume and that their diffusion time is much faster than the dynamical dynamics of binding and unbinding:

$$G(t) = \frac{1}{N}\left(\frac{1-y}{\left(1+t/\xi_{free}\right)} + \frac{y}{\left(1+t/\xi_{bound}\right)}\right) \qquad [3a]$$

where N is the number of fluorescent particles in the detection volume, y is the fraction of MS2-GFP molecules bound to the mRNA–ribosome complex, and ξ_{free} and ξ_{bound} are the diffusion times of free and bound MS2-GFP, respectively. The parameter y is a proxy to infer the RNA concentration in the single cell. Finally, Formula [3b], developed by Rigler and colleagues (23), takes into account the increase in brightness due the two *ms2*-binding sites that are present in each RNA transcript (each binding an MS2-GFP homodimer).

$$G(t) = \frac{1}{N}\frac{1}{\left[1+y\right]^2}\left(\frac{1-y}{\left(1+t/\xi_{free}\right)} + \frac{4y}{\left(1+t/\xi_{bound}\right)}\right) \qquad [3b]$$

This model can fit any experimental autocorrelation function in living *E. coli* by adjusting only two parameters, N and y. The lower limit of detection for N was about two transcripts per volume of detection.

When the RNA transcript containing the *ms2*-binding sites encoded the dsRed fluorescent protein, the self-calibration by FCS of RNA measurements from free and bound MS2-GFP was in good agreement with the simultaneous measurement of dsRed protein concentration. It is important to note that the genetic design used in this approach guarantees that only the freely diffusing mRNA transcripts that are not physically associated with an RNA polymerase or plasmid DNA are measured. To this end, the *ms2*-binding sites were located after the *DsRed* stop codon. With this orientation, the binding sites are transcribed only after *DsRed* is fully transcribed. The mRNA then becomes ‘visible’ when the MS2-GFP proteins bind to the mRNA transcript with fully transcribed *ms2*-binding sites.

1.3 Advances in FCS for single-cell measurements

Current FCS techniques require that the RNA molecules are free to diffuse. However, a recent study from Jacobs-Wagner and colleagues (24) used *in situ* hybridization to show that in *Caulobacter crescentus* and *E. coli*, chromosomally expressed mRNAs tend to localize near their site of transcription during their lifetime. This observation implies that the diffusion coefficients of chromosomally expressed mRNA are two orders of magnitude lower than mRNA molecules expressed from plasmids. When RNA transcripts are localized, imaging becomes necessary to quantify concentration (21, 25). To overcome this obstacle, wide-field FCS combines standard FCS measurements with imaging. This new experimental approach makes it possible, in principle, to quantify both freely diffusing and localized RNA molecules. The extension to wide-field FCS has become possible due to the development of new cameras that use an electron multiplying CCD technology (EMCCD). EMCCD cameras are ideal detectors because they combine speed and sensitivity with high quantum efficiency. These EMCCD cameras can be used as photon detectors, in 'kinetics mode', with only one- or two-point excitation volumes (26-27). The reading time of the pixels from the chip of the camera is far slower than the typical dead time of avalanche photon-diodes used for standard FCS single point detectors that have a dead time of about 70 ns. However, this lower temporal resolution should not be an issue for measurements in living cells because the typical timescales involved are of the order of a millisecond. Thus, the EMCCD cameras could be used to perform FCS measurements with a time resolution of 20 μs, which should suffice to determine the relevant timescales associated with molecular diffusion in cells (26-27). To improve the time resolution, Heuvelman and colleagues (28) aligned a line illumination of the sample with one line of adjacent pixels in the EMCCD chip. The physical configuration of the camera in the kinetics mode simultaneously

reads adjacent pixels from the same line and clears them within about 0.3 μs. This parallel multichannel acquisition of the fluorescence signal with an EMCCD camera improved the time resolution down to 14 μs. While FCS measurements were performed only along one dimension, this approach should also work with several contiguous lines to extend FCS measurements along the two dimensions with a sub-millisecond resolution. Wide-field FCS will most likely be immediately applicable to small rod-shaped bacteria, such as *E. coli* or Salmonella. For thicker eukaryotic tissue and cells, it is also necessary to scan along the z-axis. To expand FCS technique to higher throughput measurements along the z-axis, Needleman and colleagues (29) developed a pinhole array correlation imaging technique based on a stationary Nipkow disk and an EMCCD. While this technique has not been tested on live cells, it has the potential power to perform hundreds of FCS measurements within cells thicker than bacteria, with high temporal resolution.

2 Spectral analysis of molecular activity fluctuations to infer chemical rates

2.1 A practical aspect of the Langevin equation

There exists a phenomenological stochastic equation called the Langevin equation that describes in a general way the fluctuations of a mass-spring system in a viscous fluid, with spring constant k_{spring}, damping constant γ, and fluctuating random force $f(t)$. When the Reynolds number is low, there is no acceleration, and friction (γ) dominates the dynamics of the particle's position $x(t)$:

$$\gamma\dot{x} = -k_{spring}x + f(t) \quad [4]$$

This model has been found to be very useful to interpret, in the regime of linear approximation, the behavior of a large range of dynamical systems. For example, we will see that this model can be extended to study of biochemical reactions taking place in cells.

Taking the Fourier transform of the Langevin equation allows us to calculate the power spectrum of the fluctuations of the position δx at equilibrium:

$$\delta x^2(\omega) = \frac{2KT}{\gamma(\omega_c^2 + \omega^2)} \quad [5]$$

In the classic Langevin equation, the amplitude of the spontaneous fluctuations (D) defined with $\langle f(t) f(t') \rangle = D\delta(t - t')$ is obtained using the equipartition theorem that couples the thermal energy KT, and the energy stored in the spring given by:

$$KT = k_{spring} \langle \delta x^2 \rangle_{time} \quad [6]$$

$\langle f(t) f(t') \rangle = D\delta(t - t') = 2KT\gamma\delta(t - t')$, where T is the temperature and K is the Boltzmann constant. Formula [5] has several practical applications. For example, it is particularly useful to evaluate the sensitivity range of a mechanical transducer used in single molecule experiments. In such experiments, the mechanical transducer can be the cantilever of a force microscope, a glass fiber, or the trap formed by an optical tweezers that senses the motion of a small bead submerged in solution. To determine whether to use a stiff or soft cantilever for a given experiment, one can plot the power spectrum of the fluctuations of the cantilever's position. Spontaneous fluctuations of the mechanical transducer induced by the thermal noise are not distributed uniformly over all frequencies. The fluctuations die out for frequencies larger than the typical corner frequency

$\omega_c = \frac{k_{spring}}{\gamma}$. If the transducer becomes stiffer, the spontaneous fluctuations will spread over higher frequencies because the corner frequency $\omega_c = k/\gamma$ becomes larger. Most importantly, the thermal energy stored in the system remains constant $\left\langle \delta x^2 \right\rangle_{time} = \frac{KT}{k_{spring}}$, which represents the total area defined by the power spectrum $\left\langle \delta x^2 \right\rangle = \int_0^{+\infty} \frac{2KT}{\gamma(\omega_c^2 + \omega^2)} d\omega$. In other words, this constraint implies that the amplitude of the spontaneous fluctuations of a stiff spring will be smaller at lower frequencies than those of a softer spring (Figure 1). If the signal we plan to measure is in a lower frequency range, then a stiffer mechanical transducer will exhibit a lower background noise in this frequency range but the sensitivity of the transducer will be reduced by the same amount (30). Thus, reducing the stiffness of the transducer does not improve the signal-to-noise ratio. By contrast, reducing the dimension of the transducer will reduce the friction coefficient γ, which, in turn, will increase the corner frequency $\omega_c = k/\gamma$. So at equal stiffness, the background noise can be reduced by using transducers with smaller dimensions. Using this analysis, it was found that the force-extension measurements of a single DNA molecule are less noisy using an optical trap (31-32) with sub-micron latex beads, than using micro-glass fibers that are several micron long transducers (33).

2.2 Measuring noise to infer the sensitivity of a chemical system

For kinetic reactions, the positional coordinates $x(t)$ of the elastic spring corresponds to the concentration. Using the equation describing the fluctuations in a mass-spring system, Bialek and Setayeshgar introduced a model to describe the dynamics associated with the binding and

unbinding of a ligand to a receptor at equilibrium in a thermal bath (34). This case study is thought to be general because the fluctuations of receptor occupancy are governed solely by thermal noise. This assumption allows the authors to use the fluctuation-dissipation theorem (FDT) as a framework to relate the amplitude of the fluctuations to the macroscopic behavior of the receptor described by a kinetic equation. In the Bialek-Setayeshgar model, fluctuations in receptor activity reflect the fluctuations in the rates k^+ and k^- associated with the binding and unbinding of the ligand to the receptor. This approach is similar to that of a spring that is submerged in a thermal bath (Section 2.1). The only difference lies in the constraints that define the amplitude of the fluctuation D in the Langevin equation. The fluctuations of the rates k^+ and k^- are related to the fluctuations of the associated free energy that define the two receptor states. Using this noise analysis, they determined the sensitivity range of sample receptor. Their analysis is analogous to that of the mechanical transducers in section 2.1.

Similarly, the fluctuations in chemical reactions can yield information about the typical chemical rates governing the reactions. In the simplest example of an isomerization reaction, a molecule switches back and forth between an active and inactive state:

$$A \underset{k^-}{\overset{k^+}{\rightleftharpoons}} A^* \qquad [7]$$

where A and A* are the concentration of the inactive and active forms, and k^+ and k^- are the respective reaction rates from the inactive to active and the active to inactive form. The concentration of A^* changes such that

$$\dot{A}^*(t) = k^+ A(t) - k^- A^*(t) \qquad [8]$$

We linearize about the steady-state using

$$A^*(t) = \overline{A^*} + \delta A^*(t)$$

$$A(t) = \overline{A} + \delta A(t)$$

$$k^+(t) = k^+ + \delta k^+(t)$$

$$k^-(t) = k^- + \delta k^-(t)$$

and Equation [8] becomes

$$\delta \dot{A}^* = \delta k^+ \overline{A}^* - \delta k^- \overline{A} + \left(k^+ + k^-\right)\delta A^*$$

The rates are related by the difference of the free energy ΔF between the active and inactive states, such that $\frac{k^+}{k^-} = e^{\frac{\Delta F}{KT}}$. Using this relationship, the fluctuations of the rates are given by

$$\frac{\delta k^+}{k^+} - \frac{\delta k^-}{k^-} = \frac{\delta F}{KT}$$

and, Equation [8] takes the usual Langevin form:

$$\delta \dot{A}^*(t) = (k^+ + k^-)\delta A^*(t) + \frac{k^+ \overline{A}}{KT}\delta F(t) \qquad [9]$$

The Langevin equation [9] is analogous to the equation describing fluctuations of a mass-spring system (Equation [4]). To apply the FDT, it is convenient to Fourier transform Equation [9]:

$$\left[\frac{KT}{k^+ A^*} i\omega - \frac{k^+ + k^-}{k^+ \overline{A}^*}\right]\delta \widetilde{A}^*(\omega) = \delta \widetilde{F}(\omega)$$

The Fourier transform is defined with $\delta\widetilde{A}^*(\omega) = \int_0^\infty \delta A^*(t) e^{i\omega t} dt$ and the response function $\chi(t)$ determines the linear response ΔA^* to a small external perturbation δF such that

$$\Delta A^*(t) = \int_0^\infty \chi(t')\delta F(t-t')dt'$$

$$\Delta\widetilde{A}^*(\omega) = \widetilde{\chi}(\omega)\delta\widetilde{F}(\omega)$$

the response function becomes:

$$\widetilde{\chi}(\omega) = \frac{\delta\widetilde{A}^*(\omega)}{\delta\widetilde{F}(\omega)} = \frac{k^+\overline{A}^*}{KT\left[i\omega - k^+ + k^-\right]} \quad [10]$$

applying the FDT:

$$P_{\delta A^*}(\omega) = \frac{2KT}{\omega}\,\mathrm{Im}\left[\widetilde{\chi}(\omega)\right] \qquad [11]$$

Equation [10] becomes

$$p_{\delta A^*}(\omega) = \frac{2k^+\overline{A}^*}{[\omega^2 + (k^+ + k^-)^2]} \quad [12]$$

Plotting the power spectrum is a convenient way to study the output fluctuations of a system. The corner frequency of the power spectrum in a log-log plot gives a measure of the sum of the rates, and its integral from 0 to infinity yields the total variance of the noise of this isomerization reaction (Eq. 7):

$$\left\langle (\delta A^*)^2 \right\rangle = \int_0^{+\infty} P_{\delta A^*}(\omega)\frac{d\omega}{2\pi} = \frac{2k^+\overline{A}^*}{2\pi}\int_0^{+\infty}\frac{\tau^2 d\omega}{1+(\tau\omega)^2}$$

Therefore the total variance is:

$$\left\langle \left(\delta A^*\right)^2 \right\rangle = \frac{k^+ \overline{A}^*}{(k^+ + k^-)} \quad [13]$$

In this approach (34), there is no assumption about the underlying statistics that govern switching between A and A^*. Instead, it relies on thermodynamic equilibrium and the use of the FDT. While this approach is powerful to describe in vitro systems where thermodynamic equilibrium can be well-defined, we cannot directly extend it to living cells because they are open systems and they are far from thermodynamic equilibrium. In Section 3, we will discuss novel experimental and theoretical approaches used to describe the linear response of living cells to a small stimulus based on an extension of the FDT.

2.3 Modeling cell-to-cell variability from the noise of single gene expression in living cells- the static case

It also is now common to use the Langevin equation (35) to characterize the expression noise of a single gene (8-9). While the Langevin model yields results equivalent to that of Monte Carlo simulations, its power lies in its straightforward physical interpretation that is often obscured in numerical simulations. One standard way to deal with the stochastic aspect of chemical reactions is to assume that each coordinate of a given chemical system independently obeys Poisson statistics for which the variance and average are equal, the molecular system is well mixed, and concentrations are continuous variables. For example, Ozbudak and colleagues (8) characterize the transcription of a single gene within a cell using a simple model: $\frac{d}{dt} RNA = k_{txn} - \gamma RNA + \eta_{txn}$,

where the number of mRNA molecules, RNA, is a continuous quantity, γ is the degradation rate of RNA, k_{txn} is the transcription rate per DNA, and η_{txn} is a random function that models the noise associated with transcription. This Langevin equation assumes that there exists a steady state and that fluctuations about the steady concentration δRNA reflect the response of the system to a Gaussian white noise source, $\langle \eta_{txn}(t) \rangle = 0$ and $\langle \eta_{txn}(t)\eta_{txn}(t+\tau) \rangle = D\delta(\tau)$, where backets represent population averages, and δ represents the Dirac δ-function. Expanding around this steady-state, $\langle RNA \rangle = \frac{k_{txn}}{\gamma}$, by setting $RNA = \langle RNA \rangle + \delta RNA$ gives the Langevin equation for δRNA:

$$\frac{d}{dt}\delta RNA + \gamma \delta RNA = \eta_{txn}(t) \quad [14]$$

Fourier-transforming this equation gives $\frac{\delta RNA(\omega)}{\eta_{txn}(\omega)} = \frac{1}{\gamma + i\omega}$, $\langle |\eta_{txn}(\omega)|^2 \rangle = D$, so that the variance of the fluctuations is given by $\langle \delta RNA^2 \rangle = \int \frac{d\omega}{2\pi} \frac{1}{\gamma^2 + \omega^2} D = \frac{D}{2\gamma}$. Although this system is not at thermodymic equilibrium and we cannot use the equi-partition theorem, we can determine the value of D by assuming Poisson statistics for the fluctuations δRNA. Therefore, setting $\langle \delta RNA^2 \rangle = \langle RNA \rangle$ yields the amplitude of the input white noise $D = 2k_{txn}$ (8). Unlike in the Bialek-Setayeshgar model (Section 2.2), we cannot invoke the FDT because this system is not at thermodynamic equilibrium. In this static approach, there is usually no need to define the response function because, in general, the goal of these studies is to evaluate the variance associated with the transcription or translation of a specific gene. In other words, they aim to

measure the cell-to-cell variability within a clonal population of cells in a steady-state regime (9, 36).

2.4 The power of time-series to characterize signaling in single cells

Because it is experimentally simpler, most experimental studies typically describe the noise of biological systems as cell-to-cell variability (8-9), see Section 2.3. Such studies assume that biological systems are ergodic, that is, the temporal average at the single cell level is equal to the ensemble average across many cells at a fixed time point. Experimentally, this assumption implies that a snapshot of a population of cells at steady state can reveal the statistics of the system. However, this assumption is not always sufficient because the snapshot approach does not allow us to characterize the temporal correlations in protein fluctuations taking place within the individual cell. Thus, due to the difficulty of such experiments, only a few experiments have used time-series analysis to determine noise from a single gene (10, 25, 37-38). For example, to distinguish which genes within a transcriptional network have an active regulatory connection, Dunlop and colleagues characterized the cross-correlation of the spontaneous fluctuations in the activity of two promoters, *galS* and *galE*, in the galactose metabolism system in *E. coli* (10). A copy of each promoter controlling the expression of either CFP or YFP was integrated into the chromosome. It is not obvious that the cross-correlation would reveal interactions between the two genes because global noise would also simultaneously affect the activity of both promoters. However, there exists a time lag in the profile of the cross-correlation function between promoters that have active and inactive transcriptional interactions (here a feed-forward loop (39)). Therefore, time lags in cross-correlation functions can distinguish the uniform effect of

global extrinsic noise from the specific cases of active regulatory interactions. While this lag time is measurable by performing the cross-correlation of the activity of two promoters, it also requires that the difference between the maturation times of CFP and YFP is small enough compared to the lag induced by the regulatory interactions.

Beyond gene expression, spectral analysis has been used to analyze the nature of the temporal fluctuations throughout the signaling cascade of the chemotaxis system in *E. coli*. This system governs the locomotion of bacteria and allows the cells to move towards the source of chemical attractants, such as amino acids (40). In *E. coli*, chemotaxis has become a canonical system for the study of signal transduction networks because this network involves few components, it is amenable to tractable quantitative analyses. It exhibits, however, complex behaviors, such as sensitivity to stimulus and adaptation to environmental changes (see chapter Chemotaxis). The activity of the chemotaxis kinase CheA directly reflects environmental changes in the neighborhood of the bacterium. For example, following a sudden increase in aspartate concentration in the environment, aspartate will bind to Tar receptors, which will induce a drop of activity of the kinase CheA. For the sake of simplicity, we will assume that CheA, can be either in an active (A) or inactive state (A^*) (Figure 2). When the kinase is active, it transfers a phosphate group to the diffusible signaling response regulator CheY. Active CheYp binds to the basal part of the rotary motor that powers the rotation of a long flagellar filament and increases the probability of the motor to rotate in a clockwise (CW) direction. In swimming bacteria, clockwise (CW) rotation induces tumbles and CCW smooth runs. In the absence of a stimulus, the bacterial motor switches randomly between CCW and CW rotations, whose frequency reflects the steady-state activity of the kinase and randomizes the trajectory of a swimming cell. To summarize, a drop in kinase activity, caused by a sudden stimulus of aspartate, induces CCW

rotation of the motor (smooth run) and bias the random trajectory of the cell toward gradient of attractant. After its initial drop, the kinase activity adapts back to its pre-stimulus level. This adaptation mechanism is governed by two antagonistic enzymes, CheR and CheBp, which regulate the activity of the kinase-receptor complexes (Figure 2) (41). The standard assumption is that non-stimulated cells that are exposed in a steady environment would exhibit a steady behavior. A single-cell analysis revealed that the slow fluctuations in CheA activity were reflected in the switching behavior of a single motor (42). Power spectra were used to analyze the fluctuations of the stochastic switching events of individual motors between two states. According to Equation [15],

$$M_{CCW} \underset{k^-}{\overset{k^+}{\rightleftharpoons}} M_{CW} \quad [15]$$

the common expectation for constant rates k^+ and k^- is that the power spectrum associated with the fluctuations δM_{CW} should exhibit a Lorentzian profile. This power spectrum, identical to that of Section 2.2 (Equation [12]), would exhibit at long timescale a flat profile in a log-log plot:

$$p_{M_{CW}}(\omega) \sim \frac{1}{[\omega^2 + (k^+ + k^-)^2]} \quad [16]$$

Surprisingly, for bacteria in a steady environment, such as motility medium that does not support growth, the spectrum exhibits a corner frequency at short timescale (~1 sec), followed by a growing profile that ranges from ~10 sec to ~15 min. The slope of the power spectrum at long timescale indicates that the CCW and CW intervals from the motors are not exponentially distributed. Interestingly, the fluctuations of CheA activity are directly reflected in the

distributions of runs and tumbles of an individual bacterium. Therefore, the switching events are not governed solely by the Poisson statistics of the motor but also by an additional process that takes place in the signaling cascade and that occurs at much longer timescale. The complex profile (Figure 3) can be understood as the superimposition of two Lorentzians, one representing the motor switching with a knee frequency at short timescale and another one with a knee frequency at a much longer timescale due to the fluctuations of the CheA kinase activity governed by the slow antagonistic action of CheR and CheBp (Figure 2). As a consequence, different relative expressions of CheR or CheBp concentrations would yield different amplitudes of the fluctuations of CheA activity at long timescales. The CheR/CheBp ratio controls the amplitude of an adjustable source of behavioral variability (42). By contrast, population measurements found that the distribution CCW and CW were exponentially distributed, which would yield the power spectrum described by equation 16 without long timescale fluctuations observed at the single cell level (43). This discrepancy exemplifies the non-ergodic nature of some biological systems for which the analysis of long time series in individual cells is essential.

3 Relationship between fluctuations and response, extending the FDT to living cells

None of the previous examples has addressed the dynamical aspect of the FDT that relates spontaneous fluctuations with the linear response of a system to small external perturbation. Instead, this theorem has only been used to evaluate the variance associated with cell-to-cell variability within isogenic populations at a given time point. The next section explores whether the spontaneous fluctuations in biological systems is related to the response to a small external perturbation as predicted by the FDT.

3.1 Violation of the FDT due to energy consuming mechanisms

A classic example of experimental violation of the fluctuation-dissipation theorem uses hair-bundles from bullfrogs (12).

$$\chi(t) = -\beta \frac{d}{dt} C(t) \text{ [18]}$$

While the theorem relates the response function to the derivative of the autocorrelation function, it is often more convenient to use its formulation in the frequency space:

$$\widetilde{C}(\omega) = \frac{2}{\beta\omega} \mathrm{Im}\,\widetilde{\chi}(\omega) \text{ [19]}$$

where $\mathrm{Im}\,\widetilde{\chi}(\omega)$ is the imaginary part of the Fourier transform of the response function, which represents the dissipation of the system, and the function $\widetilde{C}(\omega)$ is the power spectrum of the spontaneous fluctuations. In physics, β^{-1} would represent the equilibrium temperature of the environment for the system. When the system departs from the equilibrium due to a mechanism that consumes energy, the theorem is violated. A standard measure of the degree of violation of the theorem is provided by the ratio between the temperature of the system and an effective temperature $T_{eff}(\omega)$:

$$\frac{T_{eff}(\omega)}{T} = \frac{\omega\beta}{2} \cdot \frac{\widetilde{C}(\omega)}{\mathrm{Im}\,\widetilde{\chi}(\omega)} \text{ [20]}$$

If this ratio is equal to unity, the theorem is satisfied. When the relationship is less than unity, the system contains an active mechanism that consumes energy, and the theorem is violated. Using Equation [20], Martin et al. compared the spontaneous fluctuations of a hair-bundle from bullfrog to its response to a sinusoidal mechanical stimulation. To demonstrate that the theorem

was violated (12) (Figure 4), they showed how far the ratio $\frac{T_{eff}(\omega)}{T}$ deviated from the unity. They concluded that the random fluctuations of hair cells are not solely due to the effect of thermal energy but also to an active mechanism within the hair cells. Such mechanism could govern active filtering and sharp frequency selectivity in this hearing system. In living systems, where there exist many energy consuming mechanisms, it is expected that the FDT is violated.

3.2 The Prost-Joanny-Pandaro fluctuation-response theorem and its application to molecular motors

A recent theoretical analysis of the FDT demonstrated that if a system has a well-defined steady state with Markovian dynamics, the FDT is extensible to a fluctuation-response theorem even in the absence of thermodynamic equilibrium (11). This result is extremely relevant to living cells that are not at thermodynamic equilibrium. Many biological systems display a well defined steady-state and exhibit fluctuations that are caused by underlying Markovian dynamics. Here, the term Markovian refers to dynamic processes that have short "memory" so that they can relax fast enough to a well-defined steady state. In the Prost-Joanny-Parrando (PJP) fluctuation-response model (11), the steady-state exists when there is a well-defined probability distribution function $\rho_{ss}(c;\lambda)$ of the variables c controlled by a set of parameters λ_α. The probability distributions are associated with the potentials $\phi(c;\lambda) = -\log[\rho_{ss}(c;\lambda)]$. The PJP fluctuation-response theorem relates the response function $\chi_{\alpha\gamma}(t-t')$ to the correlation function:

$$\chi_{\alpha\gamma}(t-t') = \frac{d}{dt}C_{\alpha\gamma}(t-t') = \frac{d}{dt}\left\langle \frac{\partial\phi(c(t);\lambda^{ss})}{\partial\lambda_\alpha}\frac{\partial\phi(c(t');\lambda^{ss})}{\partial\lambda_\gamma}\right\rangle_{ss} \qquad [17]$$

This theorem is directly applicable to in vitro biological systems and, in particular, to the bullfrog hair cells (Section 3.1). As we know, the standard FDT is violated in this system. However, when the coordinates derived from the potentials ϕ are used instead of using the conventional set of variables, such as the position coordinates, the extended PJP theorem is satisfied. This theorem becomes particularly practical to identify all the slow variables of a system, which contribute to the observed fluctuations and the relaxation to a small external stimulus.

Similarly, this theorem applies to processive molecular motors (44-45) that have non-linear dynamics and do not obey energy conservation because ATP is used as a source of energy. When an optical tweezers traps a single motor, it acts like an elastic spring opposing the motor motion. As demonstrated in the PJP paper (11), the Langevin equation is a good model for describing the position of the motor $x(t)$ subject to stochastic fluctuations $\eta(t)$:

$$\dot{x}(t) = -k[x(t) - x_{ss}] + \eta(t)$$

where x(t) is the position from the center of the trap of a small latex bead that is covalently attached to molecular motor. The random function $\eta(t)$ encapsulates both the complex stochastic behavior of the motor and the effect of thermal noise:

$$\langle \eta(t) \rangle = 0\,,\ \langle \eta(t)\eta(t') \rangle = 2D\delta(t - t')$$

Here k^{-1} is the relaxation time of this system and $\sigma^2 = D/k$. In the case of a motor trapped in an optical tweezers, the potential $\phi(c;\lambda)$ has the following analytical expression:

$$\phi(x) = -\log \rho_{ss} = \frac{(x - x_s)^2}{2\sigma^2} + \frac{1}{2}\log(2\pi\sigma^2)$$

Using this potential, one can easily verify if the PJP fluctuation-response relationship (Equation [17]) is satisfied.

3.3 Conjecture: Fluctuation-response relationship and its implication on single cell behavior

While the formulation of the PJP fluctuation-response theorem is convenient for in vitro systems whose potentials can be expressed analytically, it is less useful for living cells whose potentials are not directly accessible. However, as long as the underlying dynamic processes can be approximated by Markovian statistics and the variables under study, such as the concentrations of signaling proteins or the expression level of a specific gene, have a well-defined steady state, the PJP fluctuation-response relationship should also be, in principle, valid for living organisms. Applying the PJP fluctuation-response theorem to living cells means that we can formally write down a general relationship between the spontaneous fluctuations and the response function of the system to a small external perturbation. To illustrate the potential significance of the PJP fluctuation-response theorem in living cells, we will use bacterial chemotaxis (see Section 2.4). In *E. coli*, chemotaxis is one of the few biological systems in which both spontaneous fluctuations and response to a small external perturbation can be measured with high precision from individual living cells. Such accuracy is possible because the fluctuations of switching events between CW and CCW rotation of the bacterial motor reflect the fluctuations in the concentration of the signaling protein CheYp. Therefore, the output signal of the chemotaxis network is directly measurable. Moreover, this output signal can be experimentally monitored over a long timescale with high temporal precision, and its associated variance of the noise σ^2 and correlation time τ_{cor} can be characterized by computing the autocorrelation function C(t). In this system, the exposure to a small step of attractant defines the external perturbation, and the linear response can be characterized by the response function $\chi(t)$ and its associated response time, τ_{res}. In the regime of linear approximation, it is expected that the response time and the

correlation time from the spontaneous fluctuations before stimulus are similar, but in practice, we can only expect these two times to be proportional $\tau_{cor} \alpha \ \tau_{res}$. This relationship, which is a consequence of the linear approximation alone, yields a first practical prediction that the response time can be inferred from the spontaneous fluctuations before stimulus.

If the chemotaxis system were at thermodynamic equilibrium, the standard FDT would be satisfied:

$$\chi(t) = -\beta \frac{d}{dt} C(t)$$

Additionally, the response function and the autocorrelation functions would be directly accessible from the measurements of the time series produced from the switching behavior between CW and CCW rotational states from an individual motor. However, as in the hair bundle example (12), the chemotaxis system likely violates the FDT because of the presence of energy-consuming mechanisms. Instead, we can use the PJP theorem to assume that there exists, in principle, a relationship between fluctuations and the response of the system to a small external stimulus. Alternatively, we can formally use a Langevin equation that couples the characteristics of the spontaneous fluctuations and cellular response to a small stimulus. The fluctuations of the switching behavior of individual motors are directly related to the fluctuations, δA, of the kinase activity CheA. Therefore, the behavior of the chemotaxis system can be coarse-grained by the following Langevin equation (41):

$$\dot{\delta A}^* = -\frac{1}{\tau_{cor}} \delta A + \sqrt{D} \delta \eta(t)$$

where $\sqrt{D}\delta\eta(t)$ is an input random function that has the characteristics of white noise and an amplitude D, and τ_{cor} is the measured correlation time in the output of the signaling system. In

this phenomenological model, there exists a strict relationship between the noise amplitude of the kinase activity σ^2_{CheA} and the correlation time of the system τ_{cor} such that $\sigma^2_{CheA} = \frac{D}{2}\tau_{cor}$. Importantly, because $\tau_{cor} \alpha\ \tau_{res}$, the noise σ^2_{CheA} that governs the behavioral variability is coupled to the cellular response τ_{res} through the coefficient D. The coupling coefficient D can depend on the cellular state in a very complex way. Unfortunately, we do not have access to all variables of this living system, and it is not realistic to predict theoretically how D depends on the cellular state. However, if the general PJP fluctuation-response theorem is valid, it implies, *in principle*, the existence of a coefficient D that governs the coupling between noise and response time for each cellular state. In chemotaxis, the noise of the kinase CheA is reflected in the behavioral variability of the motor behavior of a single bacterium, and the coefficient D should govern the coupling between the cellular response and the behavioral variability of bacteria as stated by the Langevin equation.

While it is difficult to evaluate how the coefficient D varies with different cellular states, it is straightforward to compute it for different concentrations of the chemotaxis proteins using a standard kinetic model of chemotaxis. For example, in a simple stochastic model, D was modeled using the fact that the adaptation mechanism is governed by a futile cycle (41). Futile cycles are ubiquitous in signaling cascades and usually consist of two catalysts acting antagonistically to regulate the activity of a kinase protein. In brief, the two catalyst enzymes act as a sort of push-pull mechanism to control the activity of the kinase CheA (46). In chemotaxis, the coefficient D represents the strength of the spontaneous fluctuations taking place within a futile cycle associated with the methylation and demethylation reactions of receptors and was explicitly calculated in Emonet and Cluzel (41):

$$D \sim b \cdot A^* + r \cdot A$$

where $b = \frac{k_b \varepsilon_{bp}}{K_b + A^*}$ and $r = \frac{k_r \varepsilon_r}{K_r + A}$, and where A^* is the concentration of free active kinase, ε_{bp} is the concentration of CheB-P, K_b is the Michaelis-Menten constant, k_b is the catalytic rate associated with demethylation and A is the concentration of free inactive kinase, ε_r is the concentration of CheR, K_r is the Michaelis-Menten constant, and k_r is the catalytic rate associated with methylation. Importantly, the coefficient D has strictly the same form as in ref. (47), where D was independently calculated for a vertebrate photo-transduction cascade. This similarity results from the fact that the same futile cycle is used as an adaptive mechanism in both signaling cascades. A wide range of other signaling pathways use similar cycles, such as Map-kinase pathways, so it is tempting to hypothesize that for most of these pathways the coupling between noise and response time should exhibit similar properties as that predicted in the chemotaxis signaling pathway. For example, in bacterial chemotaxis, we theoretically found that D varies weakly with the CheA kinase activity. As a result, we can predict that the cellular response scales linearly with behavioral variability measured before stimulus. In other words, this prediction implies that cells with the largest noise would also exhibit the longest response to a small external stimulus. It would certainly be interesting to investigate this prediction experimentally in a range of biological systems to determine when and how spontaneous fluctuations are coupled to the cellular response.

Although the discussion of this last section is highly speculative, it highlights the possibility that beyond the chemotaxis network, the PJP fluctuation-response theorem and the Langevin

equation could provide a useful and general framework to characterize how noise and cellular response could be coupled in living organisms.

Acknowledgements

This chapter reflects discussions and ongoing work with Thierry Emonet, Heungwon Park, and John Marko on the conjecture relating fluctuation and response in single cells (section 3.3), Jeff Moffitt and Calin Guet on technical advances of FCS (section 1.3) and Kevin Wood and Arvind Subramaniam on the Langevin equation (section 2.1). Wendy Grus provided editorial assistance.

REFERENCES

1. Brown, R. 1866. A brief account of microscopical observations made in the months of June, July and August, 1827, on the particles contained in the pollen of plants; and on the general existence of active molecules in organic and inorganic bodies. In The miscellaneous botanical works of Robert Brown. J. Bennett, editor. R. Hardwicke, London.
2. Einstein, A. 1905. Über die von der molekularkinetischen Theorie der Wärme geforderte Bewegung von in ruhenden Flüssigkeiten suspendierten Teilchen. Annalen der Physik 322:549-560.
3. Elson, E. L., and D. Magde. 1974. Fluorescence Correlation Spectroscopy .1. Conceptual Basis and Theory. Biopolymers 13:1-27.
4. Magde, D., E. L. Elson, and W. W. Webb. 1974. Fluorescence Correlation Spectroscopy .2. Experimental Realization. Biopolymers 13:29-61.
5. Magde, D., W. W. Webb, and E. Elson. 1972. Thermodynamic Fluctuations in a Reacting System - Measurement by Fluorescence Correlation Spectroscopy. Physical Review Letters 29:705-&.
6. Guet, C. C., L. Bruneaux, T. L. Min, D. Siegal-Gaskins, I. Figueroa, T. Emonet, and P. Cluzel. 2008. Minimally invasive determination of mRNA concentration in single living bacteria. Nucleic Acids Research 36:-.
7. Le, T. T., S. Harlepp, C. C. Guet, K. Dittmar, T. Emonet, T. Pan, and P. Cluzel. 2005. Real-time RNA profiling within a single bacterium. P Natl Acad Sci USA 102:9160-9164.
8. Ozbudak, E. M., M. Thattai, I. Kurtser, A. D. Grossman, and A. van Oudenaarden. 2002. Regulation of noise in the expression of a single gene. Nat Genet 31:69-73.
9. Elowitz, M. B., A. J. Levine, E. D. Siggia, and P. S. Swain. 2002. Stochastic gene expression in a single cell. Science 297:1183-1186.
10. Dunlop, M. J., R. S. Cox, J. H. Levine, R. M. Murray, and M. B. Elowitz. 2008. Regulatory activity revealed by dynamic correlations in gene expression noise. Nat Genet 40:1493-1498.
11. Prost, J., J. F. Joanny, and J. M. Parrondo. 2009. Generalized fluctuation-dissipation theorem for steady-state systems. Phys Rev Lett 103:090601.
12. Martin, P., A. J. Hudspeth, and F. Julicher. 2001. Comparison of a hair bundle's spontaneous oscillations with its response to mechanical stimulation reveals the underlying active process. P Natl Acad Sci USA 98:14380-14385.
13. Krichevsky, O., and G. Bonnet. 2002. Fluorescence correlation spectroscopy: the technique and its applications. Reports on Progress in Physics 65:251-297.
14. Meacci, G., J. Ries, E. Fischer-Friedrich, N. Kahya, P. Schwille, and K. Kruse. 2006. Mobility of Min-proteins in Escherichia coli measured by fluorescence correlation spectroscopy. Phys Biol 3:255-263.
15. Bacia, K., S. A. Kim, and P. Schwille. 2006. Fluorescence cross-correlation spectroscopy in living cells. Nat Methods 3:83-89.
16. Cluzel, P., M. Surette, and S. Leibler. 2000. An ultrasensitive bacterial motor revealed by monitoring signaling proteins in single cells. Science 287:1652-1655.
17. Politz, J. C., E. S. Browne, D. E. Wolf, and T. Pederson. 1998. Intranuclear diffusion and hybridization state of oligonucleotides measured by fluorescence correlation spectroscopy in living cells. P Natl Acad Sci USA 95:6043-6048.
18. Alon, U., L. Camarena, M. G. Surette, B. A. Y. Arcas, Y. Liu, S. Leibler, and J. B. Stock. 1998. Response regulator output in bacterial chemotaxis. Embo Journal 17:4238-4248.
19. Kuo, S. C., and D. E. Koshland. 1989. Multiple Kinetic States for the Flagellar Motor Switch. J Bacteriol 171:6279-6287.

20. Scharf, B. E., K. A. Fahrner, L. Turner, and H. C. Berg. 1998. Control of direction of flagellar rotation in bacterial chemotaxis. P Natl Acad Sci USA 95:201-206.
21. Bertrand, E., P. Chartrand, M. Schaefer, S. M. Shenoy, R. H. Singer, and R. M. Long. 1998. Localization of ASH1 mRNA particles in living yeast. Molecular Cell 2:437-445.
22. Golding, I., and E. C. Cox. 2004. RNA dynamics in live Escherichia coli cells. P Natl Acad Sci USA 101:11310-11315.
23. Rauer, B., E. Neumann, J. Widengren, and R. Rigler. 1996. Fluorescence correlation spectrometry of the interaction kinetics of tetramethylrhodamin alpha-bungarotoxin with Torpedo californica acetylcholine receptor. Biophys Chem 58:3-12.
24. Llopis, P. M., A. F. Jackson, O. Sliusarenko, I. Surovtsev, J. Heinritz, T. Emonet, and C. Jacobs-Wagner. 2010. Spatial organization of the flow of genetic information in bacteria. Nature 466:77-U90.
25. Golding, I., J. Paulsson, S. M. Zawilski, and E. C. Cox. 2005. Real-time kinetics of gene activity in individual bacteria. Cell 123:1025-1036.
26. Burkhardt, M., and P. Schwille. 2006. Electron multiplying CCD based detection for spatially resolved fluorescence correlation spectroscopy. Optics Express 14:5013-5020.
27. Kannan, B., J. Y. Har, P. Liu, I. Maruyama, J. L. Ding, and T. Wohland. 2006. Electron multiplying charge-coupled device camera based fluorescence correlation spectroscopy. Analytical Chemistry 78:3444-3451.
28. Heuvelman, G., F. Erdel, M. Wachsmuth, and K. Rippe. 2009. Analysis of protein mobilities and interactions in living cells by multifocal fluorescence fluctuation microscopy. European Biophysics Journal with Biophysics Letters 38:813-828.
29. Needleman, D. J., Y. Q. Xu, and T. J. Mitchison. 2009. Pin-Hole Array Correlation Imaging: Highly Parallel Fluorescence Correlation Spectroscopy. Biophys J 96:5050-5059.
30. Bustamante, C., J. C. Macosko, and G. J. L. Wuite. 2000. Grabbing the cat by the tail: Manipulating molecules one by one. Nat Rev Mol Cell Bio 1:130-136.
31. Wang, M. D., H. Yin, R. Landick, J. Gelles, and S. M. Block. 1997. Stretching DNA with optical tweezers. Biophys J 72:1335-1346.
32. Perkins, T. T., D. E. Smith, R. G. Larson, and S. Chu. 1995. Stretching of a Single Tethered Polymer in a Uniform-Flow. Science 268:83-87.
33. Cluzel, P., A. Lebrun, C. Heller, R. Lavery, J. L. Viovy, D. Chatenay, and F. Caron. 1996. DNA: An extensible molecule. Science 271:792-794.
34. Bialek, W., and S. Setayeshgar. 2005. Physical limits to biochemical signaling. P Natl Acad Sci USA 102:10040-10045.
35. Langevin, P. 1908. The theory of brownian movement. Comptes Rendus Hebdomadaires Des Seances De L Academie Des Sciences 146:530-533.
36. Swain, P. S., M. B. Elowitz, and E. D. Siggia. 2002. Intrinsic and extrinsic contributions to stochasticity in gene expression. P Natl Acad Sci USA 99:12795-12800.
37. Rosenfeld, N., J. W. Young, U. Alon, P. S. Swain, and M. B. Elowitz. 2005. Gene regulation at the single-cell level. Science 307:1962-1965.
38. Austin, D. W., M. S. Allen, J. M. McCollum, R. D. Dar, J. R. Wilgus, G. S. Sayler, N. F. Samatova, C. D. Cox, and M. L. Simpson. 2006. Gene network shaping of inherent noise spectra. Nature 439:608-611.
39. Mangan, S., and U. Alon. 2003. Structure and function of the feed-forward loop network motif. P Natl Acad Sci USA 100:11980-11985.
40. Adler, J. 1966. Chemotaxis in bacteria. Science 153:708-716.
41. Emonet, T., and P. Cluzel. 2008. Relationship between cellular response and behavioral variability in bacterial chernotaxis. P Natl Acad Sci USA 105:3304-3309.

42. Korobkova, E., T. Emonet, J. M. G. Vilar, T. S. Shimizu, and P. Cluzel. 2004. From molecular noise to behavioural variability in a single bacterium. Nature 428:574-578.
43. Block, S. M., J. E. Segall, and H. C. Berg. 1983. Adaptation Kinetics in Bacterial Chemotaxis. J Bacteriol 154:312-323.
44. Svoboda, K., C. F. Schmidt, B. J. Schnapp, and S. M. Block. 1993. Direct Observation of Kinesin Stepping by Optical Trapping Interferometry. Nature 365:721-727.
45. Visscher, K., M. J. Schnitzer, and S. M. Block. 1999. Single kinesin molecules studied with a molecular force clamp. Nature 400:184-189.
46. Goldbeter, A., and D. E. Koshland. 1981. An Amplified Sensitivity Arising from Covalent Modification in Biological-Systems. Proceedings of the National Academy of Sciences of the United States of America-Biological Sciences 78:6840-6844.
47. Detwiler, P. B., S. Ramanathan, A. Sengupta, and B. I. Shraiman. 2000. Engineering aspects of enzymatic signal transduction: photoreceptors in the retina. Biophys J 79:2801-2817.

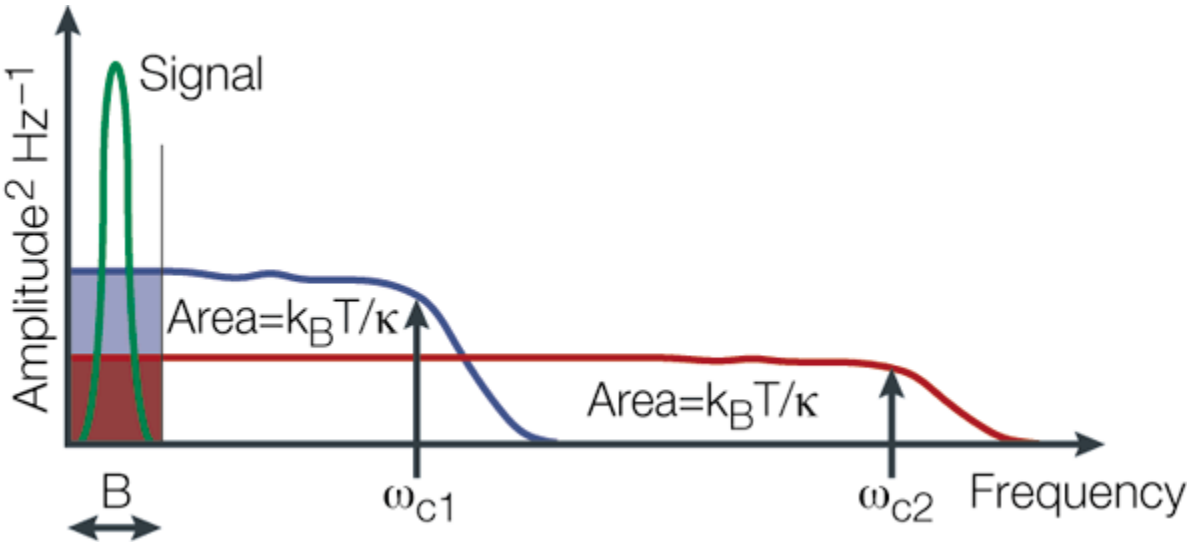

Figure 1: Thermal spontaneous fluctuations of a mechanical transducer. Changing the corner frequency, $\omega_c = k_{spring}/\gamma$, is achieved by changing the stiffness or the dimension of the mechanical transducer.

Reprinted by permission from Macmillan Publishers Ltd: [Nature Reviews Molecular Cell Biology] (Bustamante et al “Grabbing the cat by the tail: manipulating molecules one by one” 1: 130-136), copyright (2000).

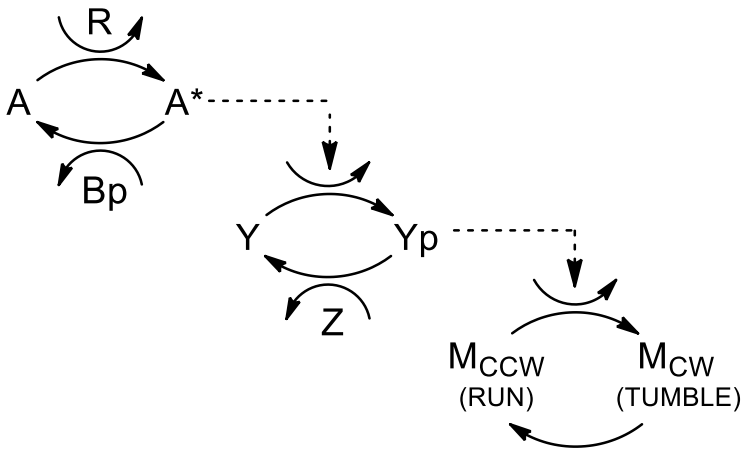

Figure 2: Receptor-kinase signaling cascade in the chemotaxis system. When ligands bind to transmembrane receptors, the receptors control the kinase CheA (*A*) activity.In its active form (A*) CheA phosphorylates the signaling molecule CheY (*Y*) into the active form CheY-P (*Y*p). CheY-P diffuses throughout the cell and interacts with the flagellar motors to induce clockwise rotation (tumble) (M_{CW}) from counterclockwise rotation (run) (M_{CCW}). The phosphatase CheZ (*Z*) dephosphorylates CheY-P. A sudden increase in ligand-binding causes a decrease in kinase activity. Two antagonistic enzymes regulate the activity of the kinase-receptor complexes. The methyltransferase CheR (*R*) catalyzes the autophosphorylation of CheA by methylating the receptors. The active kinase *A** phosphorylates the methylesterase CheB in CheB-P (*B*p). CheB-P removes methyl groups from active receptor complexes, which catalyze kinase deactivation.

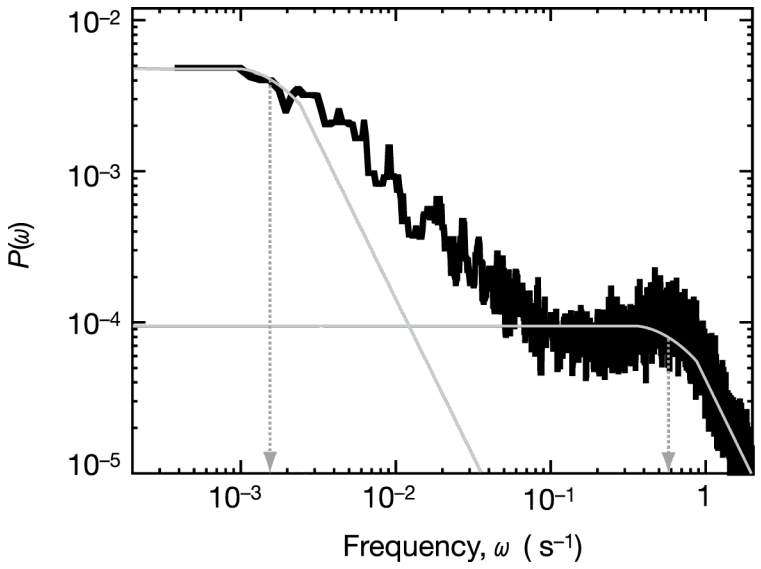

Figure 3: Noise in the chemotaxis network. (Black curve) Power spectrum of the network output from a single non-stimulated wild-type cell can be described by two superimposed Lorentzian curves (grey). The knee frequency (dashed arrows) of each Lorentzian curve comes from distinct parts of the signaling network (Fig. 1). The higher frequency is the typical time for the motor switching. The lower frequency is the typical time for the CheA kinase fluctuations. Adapted by permission from Macmillan Publishers Ltd: Nature (Korbokova et al "From molecular noise to behavioural variability in a single bacterium" 428: 574-578), copyright (2004).

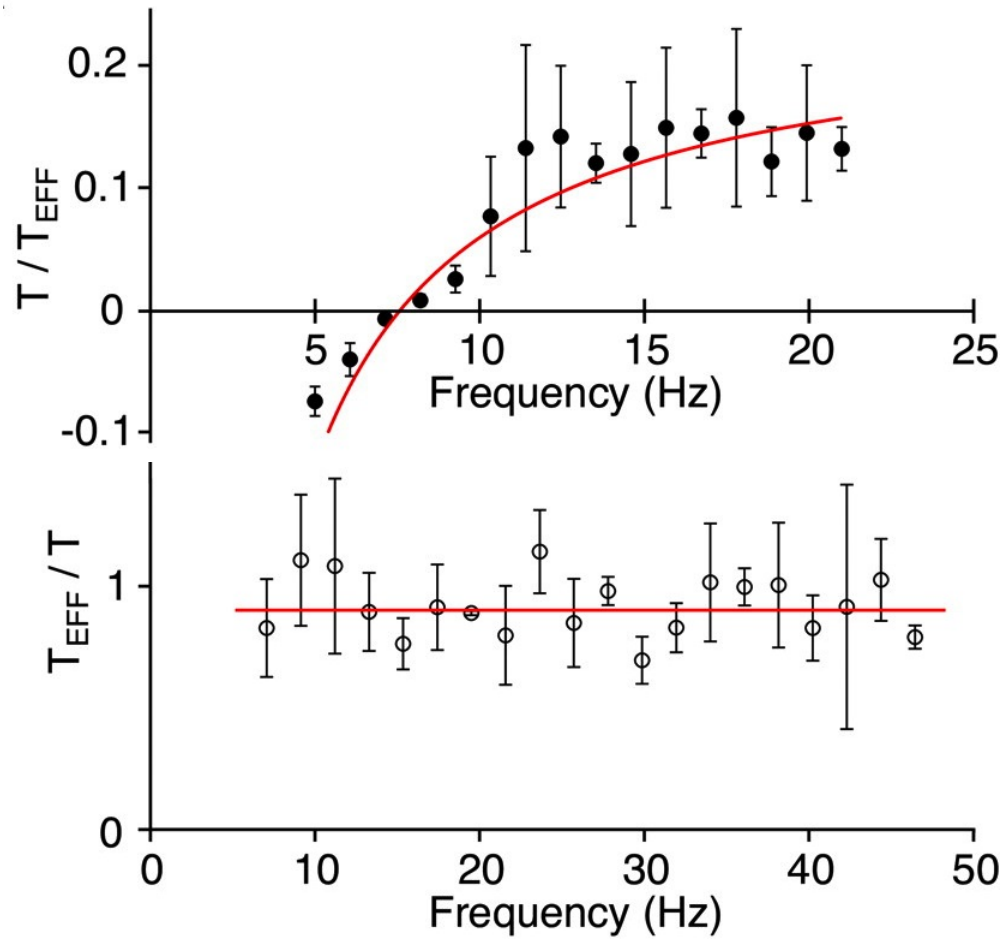

Figure 4: The effective temperature from a bundle of hair cells. Top panel: an active mechanism dissipates energy and violates the FDT. Bottom panel: When the active mechanism in the hair bundle is disrupted, the ratio $\frac{T_{eff}(\omega)}{T}$ is near unity, and FDT is satisfied. Reprinted from Martin et al "Comparison of a hair bundle's spontaneous oscillations with its response to mechanical stimulation reveals the underlying active process" 98: 14380-14385, Copyright (2001) National Academy of Sciences, U.S.A.

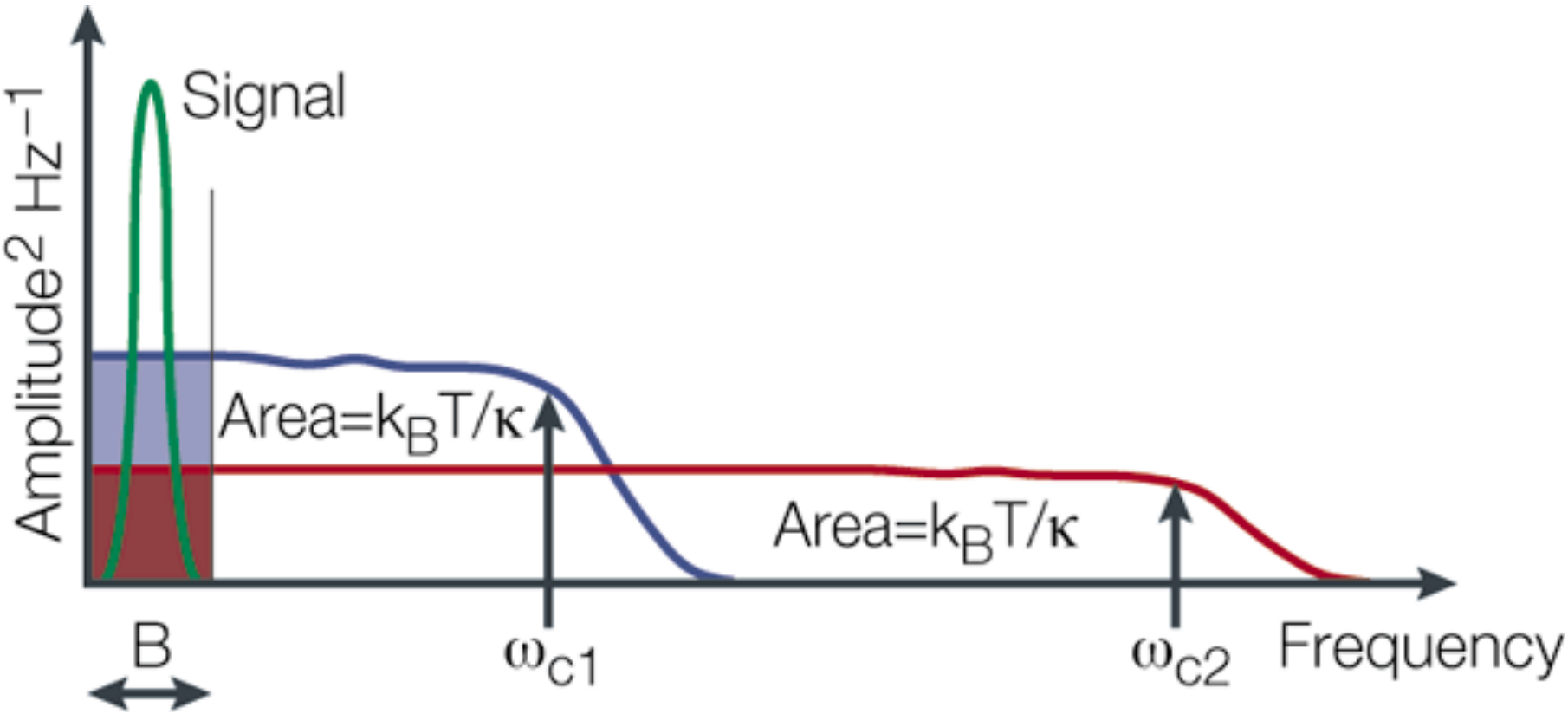
Amplitude^2 Hz^{-1}
Signal
Area=k_BT/κ
Area=k_BT/κ
B
ω_{c1}
ω_{c2}
Frequency

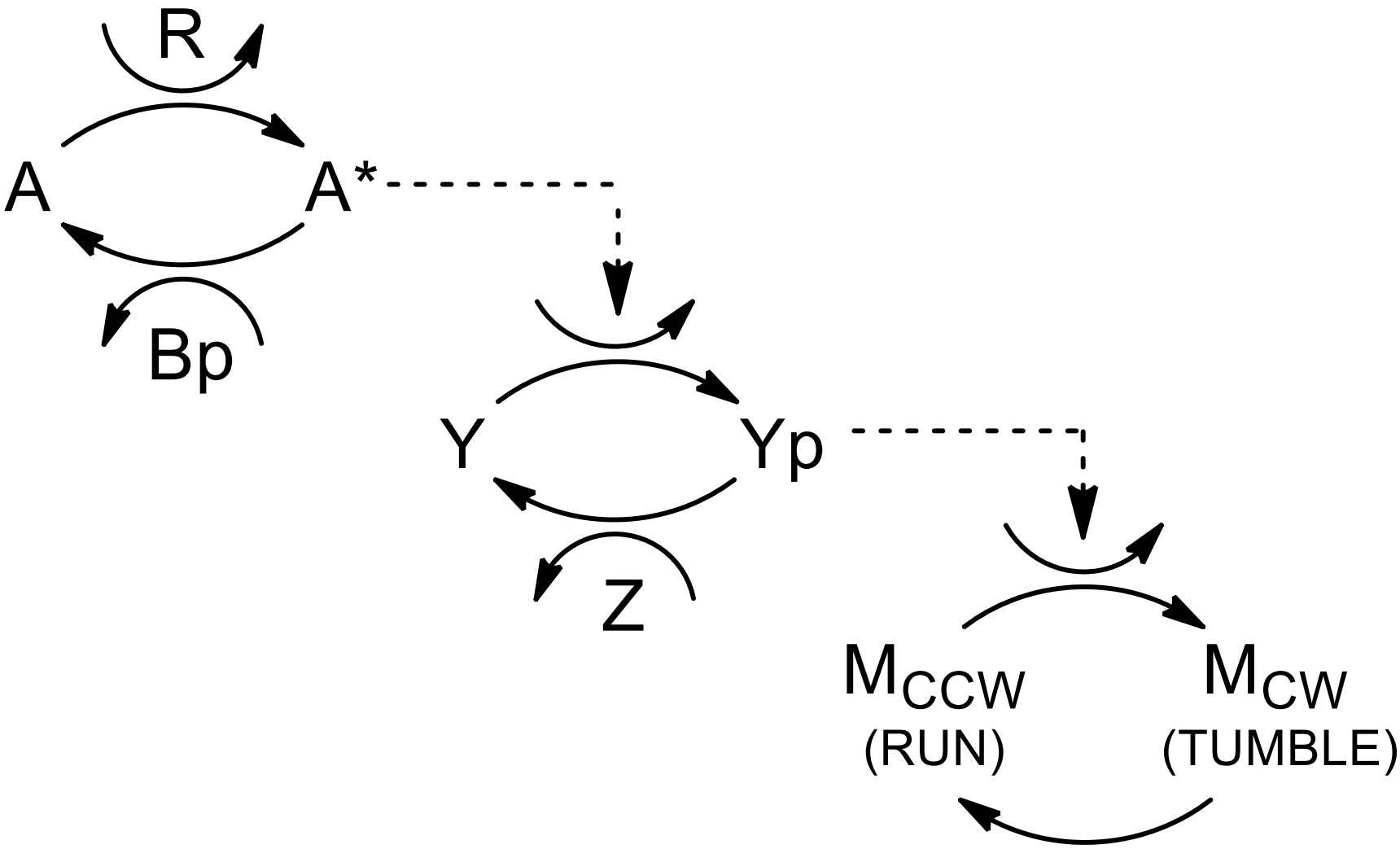
R
A
A*
Bp
Y
Yp
Z
MCCW
(RUN)
MCW
(TUMBLE)

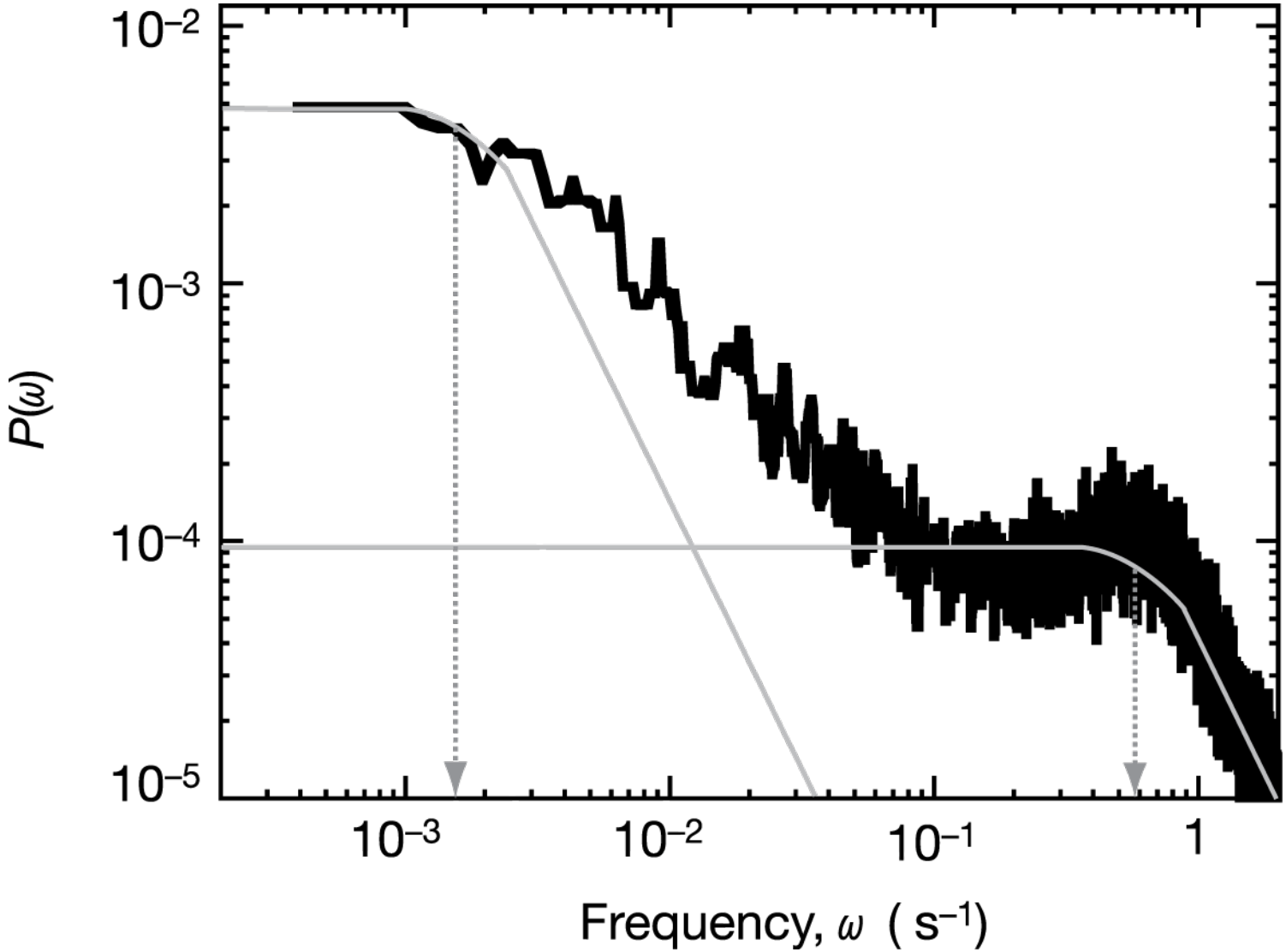
10⁻²
10⁻³
10⁻⁴
10⁻⁵
P(ω)
10⁻³
10⁻²
10⁻¹
1
Frequency, ω (s⁻¹)

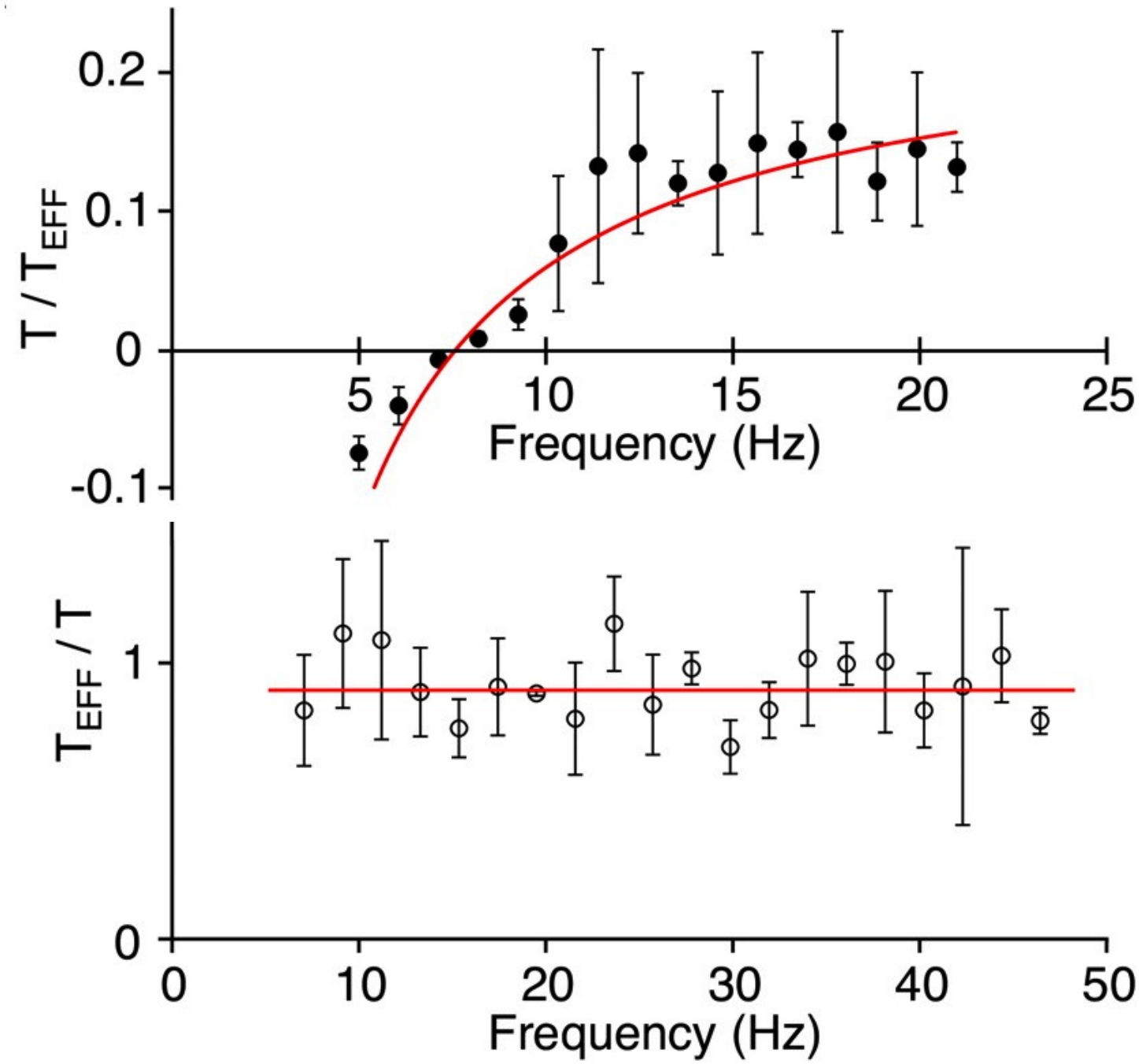
0.2
0.1
0
-0.1
T / T_EFF
5
10
15
20
25
Frequency (Hz)
T_EFF / T
1
0
0
10
20
30
40
50
Frequency (Hz)